ACS APPLIED NANO MATERIALS
Cite This: ACS Appl. Nano Mater. 2018, 1, 4401−4407
Letter
www.acsanm.org

Improving Electrical Breakdown Strength of Polymer Nanocomposites by Tailoring Hybrid-Filler Structure for High-Voltage Dielectric Applications

Bo Li,*,† Felipe Salcedo-Galan,†,‡ Panagiotis I. Xidas,†,§ and Evangelos Manias*,†

†Department of Materials Science and Engineering, The Pennsylvania State University, University Park, Pennsylvania 16802, United States

Supporting Information

ABSTRACT: In general, dielectric multifiller polymer composites have the potential to achieve enhanced performances by integrating the desirable properties of each filler. However, the improvement in thermophysical and dielectric properties is often accompanied by a deterioration of electrical breakdown strength (E_{BD}). Here, we explore a two-filler polymer nanocomposite structure, based on polyolefins with montmorillonite and calcium carbonate fillers, and present an effective approach to obtain enhanced E_{BD} by tailoring the composite morphology (by designing the pseudo-two-dimensional nanoclays to preferentially physisorb on the surfaces of calcium carbonates, so as to change the nature of the filler/polymer interfaces). It is shown that, in these structured polymer nanocomposites, the breakdown performance is substantially improved, exceeding the performance of the unfilled polymers and of the respective single-filler composites. The enhanced dielectric behavior originates from the specific composite morphology, which capitalizes on the platelet nanofillers to enhance the microfiller/polymer interfaces and on the extended hybrid-filler structure to mitigate low-energy failure initiation and propagation.

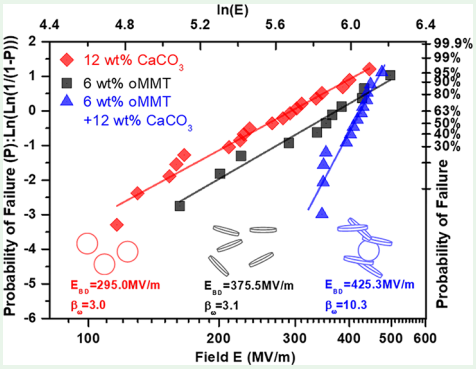

KEYWORDS: *dielectric breakdown, hybrid-filler polymer nanocomposite, structure tailoring, montmorillonite nanoclay, filler/polymer interface, polyolefin*

Polymer-based dielectrics are widely used as insulation for high-voltage systems, such as power transmission cables, high-voltage motors, high power transformers, and pulse generators, proliferating in applications due to their intrinsic high breakdown strength (E_{BD}), ease of manufacturing, and excellent mechanical flexibility at low density. Beyond good insulating performance—that is, high dielectric constant and E_{BD}, and low dielectric loss—the next-generation insulation dielectrics should also possess larger thermal conductivity, enhanced thermal stability, and higher resistance to electrical tracking, weathering, and fatigue.[1,2]

Addition of functional fillers into polymers represents a facile approach to expand the property envelope toward meeting such enhanced requirements over multiple properties. However, a common challenge underlying the composite approach is a deterioration of electrical breakdown strength (E_{BD}). Depending on the composite system, this decreased E_{BD} can be traced to the mismatch in permittivity between fillers and polymers, resulting in strong intensification and sharp distortion in local electric fields and/or to dielectrically weak interfaces (i.e., more breakdown initiation sites, higher concentrations of space charges, or lower-energy pathways for electrical failure), especially when micron-sized or high loadings of fillers are used.[3,4] To overcome this property tradeoff, innovative approaches have been explored.[5−7] One promising approach involves using insulating nanoparticles with low permittivity and high aspect ratio, such as boron nitride (BN) nanosheets,[8,9] or pseudo-two-dimensional (2D) nanoclay platelets,[10] as secondary cofiller. These nanofillers have been shown to enhance E_{BD} of the nanocomposites by providing ordered traps and scattering centers to mobile charges and by increasing path tortuosity for e^- treeing propagation.[11−13] However, studies based on such dual-filler polymer composites are less common, perhaps because the performance of these composites typically falls below expectation. In one successful example,[14] researchers employed together hexagonal BN nanosheets and $BaTiO_3$ nanoparticles to enhance both the dielectric constant and breakdown strength of the polymer nanocomposite, capitalizing on the insulating properties of BN nanofillers, the high permittivity of $BaTiO_3$, and taking advantage of filler-assisted improved dispersion. In this case, the proper design of polymer/filler and filler/filler interfaces is crucial, as also are the relative dispersions of the two fillers in the composite. In opposite cases, in systems with nonoptimal interface design, composites yield far smaller property improvements, even if the filler/filler

Received: July 3, 2018
Accepted: August 29, 2018
Published: August 29, 2018

DOI: 10.1021/acsanm.8b01127
ACS Appl. Nano Mater. 2018, 1, 4401−4407

Scheme 1. Schematic Representation of the Fillers, and the Two-Filler Structure in the Hybrid-Filler Composites

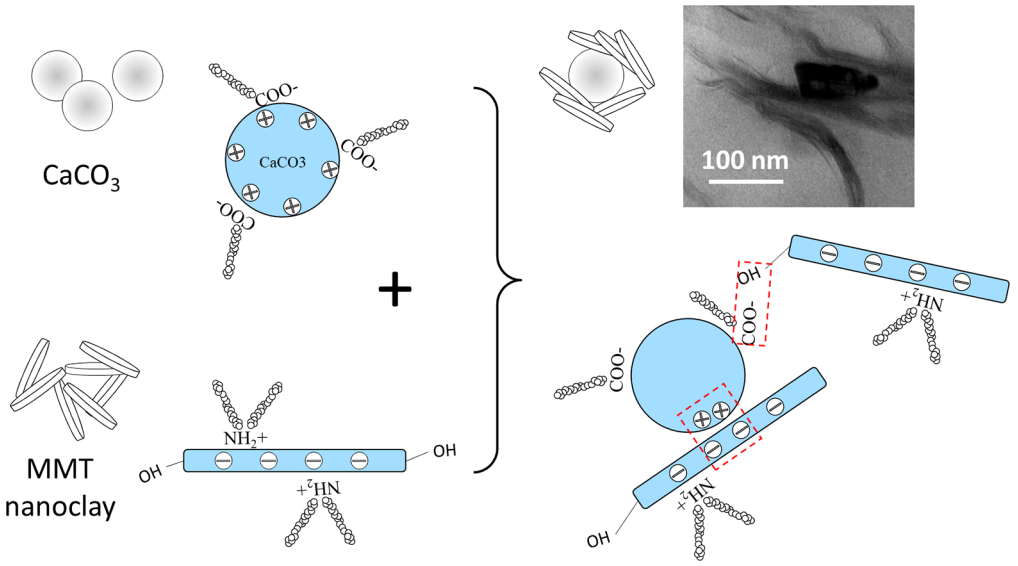

structures and the composite morphologies are the same. For instance, epoxy composites with nanoclay/$BaTiO_3$ failed to achieve markedly improved E_{BD},[15,16] although the composites had similar composite morphologies as the BN/$BaTiO_3$ composites above.

Here we present an approach to enhance the high field endurance of multifiller polymer composites by tailoring the hybrid-filler structure so as to improve the filler interfaces. Since the electrical failure in such polymer/ceramic composites is initiated primarily from the dielectrically weak interfaces,[17,18] controlled filler dispersion, with the addition of a second-type of insulating nanofillers predominantly located at the poor interfaces of the first filler, could prevent localized breakdowns, leading to improved breakdown strength. Toward this end, structured nanocomposites based on calcium carbonate ($CaCO_3$) and montmorillonite (MMT) are prepared, in which the surfaces of $CaCO_3$ are covered by physisorbed MMT nanofillers, to reinforce the $CaCO_3$/polymer interface. The particular dual-filler arrangement in the composites is expected to maintain the property improvements imparted by the microfiller and, at the same time, enhance electric field endurance by shielding the dielectrically weak interfaces. MMT layered nanosilicates are selected, because they have a high aspect ratio (pseudo-2D), good electrical insulating and barrier properties, and are shown to be effective in improving the breakdown strength of polyolefin nanocomposites.[10,19] $CaCO_3$ microfillers are commonly employed in polyolefin composites to improve the thermal conductivity, mechanical properties, and solvent resistance of the composites;[20] besides, these polar particles show strong adhesion to the organoclays, promoted by their favorable dipolar interactions (the surface dipoles of $CaCO_3$ are oriented antiparallel to those of the nanoclays; Scheme 1). Furthermore, all components of the composite have similar dielectric constants (cf. $\kappa_{polymer} \approx 2$, $\kappa_{MMT} \approx 4$, $\kappa_{CaCO3} \approx 6$), which allows for the decoupling of morphology from field enhancement and provides a clearer understanding of the effect of morphology on the mitigation of electric-failure propagation.[21]

The dual-fillers' structure and their distribution within the polymer matrix are directly observed by transmission electron microscopy (TEM; Figure 1a–d), and the local dispersion of organomontmorillonite (oMMT) nanoclays is further assessed by X-ray diffraction (XRD; Figure 1e). The prescribed morphology for the hybrid filler is achieved in the structured

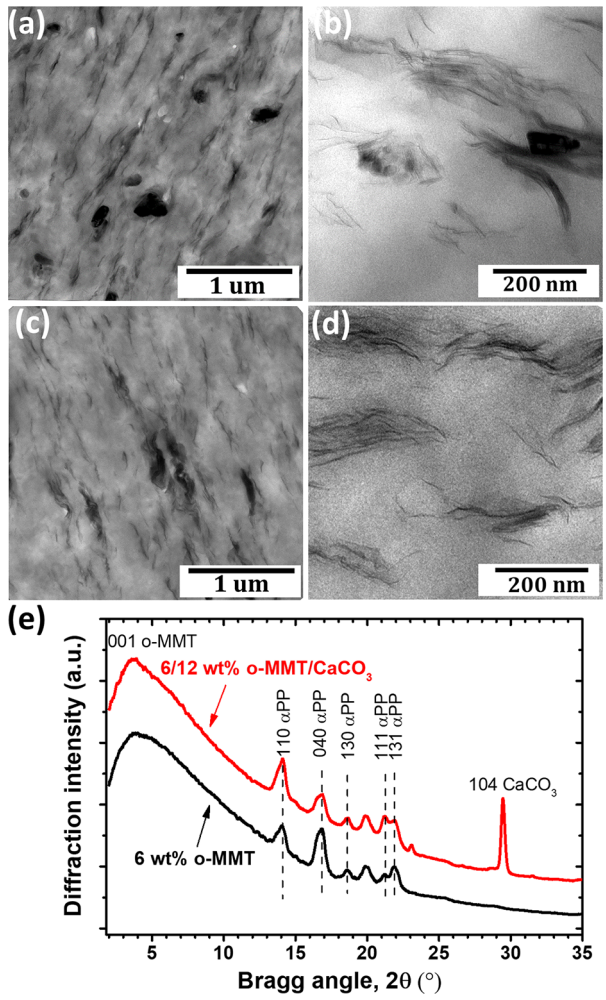

Figure 1. TEM images of the nanocomposites: (a, b) with both oMMT and $CaCO_3$ and (c, d) with only oMMT. (e) XRD measurements of the single-filler and dual-filler nanocomposite.

DOI: 10.1021/acsanm.8b01127
ACS Appl. Nano Mater. 2018, 1, 4401–4407

nanocomposite, as shown in Figure 1a and more clearly in Figure 1b. Namely, almost all $CaCO_3$ particles are decorated by the oMMT nanofillers, which are physisorbed on the surface of $CaCO_3$ due to the favorable interactions between the polar $CaCO_3$ particles and the negatively charged silicates.[22] The controlled arrangement of the two fillers could be further stabilized when the organic modifiers of the $CaCO_3$, alkyl-carboxyls, react with the hydroxyl groups remaining on the surface of the oMMT nanoclays (Scheme 1). Apart from the hierarchical structure formed by the two fillers, both dual-filler composite (Figure 1a) and single-filler composite (Figure 1c) demonstrate uniform filler distribution at the micron scale. At the nanometer scale, the organoclays assume an intercalated/exfoliated mixed morphology in both types of composites (Figure 1b,d). Specifically, a plethora of smaller MMT platelets is well-exfoliated, while the larger MMT layers are stacked in polymer-intercalated tactoids consisting of tens of layers. This is also the structure reflected from the XRD measurements. As presented in Figure 1e, both composites exhibit a signature polyolefin/oMMT intercalation diffraction pattern, with a broad 001 MMT diffraction peak showing at the Bragg angle $2\theta \approx 3.7-3.8°$, corresponding to an average intergallery spacing of 23−24 Å; moreover, the 001 MMT peaks of these two composites are similarly broad, implying a similar size for the intercalated tactoids; that is, the average number of clay layers in the intercalated stacks is comparable in both composites. The second-order 002 MMT peak is absent, indicating good dispersion at the multiple-filler length scale (disordered fillers, or swelling of tactoids), which is also consistent with the increased background at near-0 diffraction angles.

To confirm that the specific architecture of the hybrid filler is beneficial for the high field properties of the polymer composites, the dielectric breakdown of the nanocomposites is analyzed by a two-parameter Weibull distribution function (eq S1). Since the dispersion of nanoclays in nonpolar polypropylene (PP) requires the use of Mah-functionalized PP (PP-Mah),[23] composites with different nanoclay contents have different polymer-matrix compositions (i.e., ratio of PP-Mah to PP); the dielectric breakdown of polymer controls (polymer blends with the same polymer compositions as the composites) is also studied here, to accurately quantify the effects of the fillers beyond any contributions of the polymer matrix.

Figure 2 presents the Weibull plots of the polymer composites containing the hybrid fillers and the single fillers, respectively, as well as the respective polymer controls; the measured Weibull parameters are also summarized in Figure 3 and Table 1. Superior high field performance of the structured hybrid nanocomposites over the unfilled polymers and the single filler composites is clearly demonstrated. As shown in Figure 3a, the characteristic breakdown strengths (E_{BD}, corresponding to an applied field at 63.2% failure probability, eq S1) of the polymer is decreased when the 12 wt % $CaCO_3$ particles are introduced, but it can be enhanced with the addition of 6 wt % oMMT nanoclays. For the structured dual-filler composites, controlling the distribution of the nanoclays primarily at the $CaCO_3$ interfaces effectively improves E_{BD} of the $CaCO_3$ composite, which probably is intuitively expected; but what is not expected is that the breakdown performance of these structured nanocomposites surpasses even that of the oMMT composite, despite the presence of the dielectrically unfavorable $CaCO_3$ microparticles. For instance, the incorporation of 6 wt % oMMT and 12 wt % $CaCO_3$ leads to a 25% increase in E_{BD}, exceeding the contribution from the addition of nanoclay or calcium carbonate alone. In the latter case of the single-filler composites, only an 11% E_{BD} increase can be achieved in the oMMT composite with the same 6 wt % oMMT addition, and E_{BD} is reduced by 13% in the 12 wt % $CaCO_3$ composite.

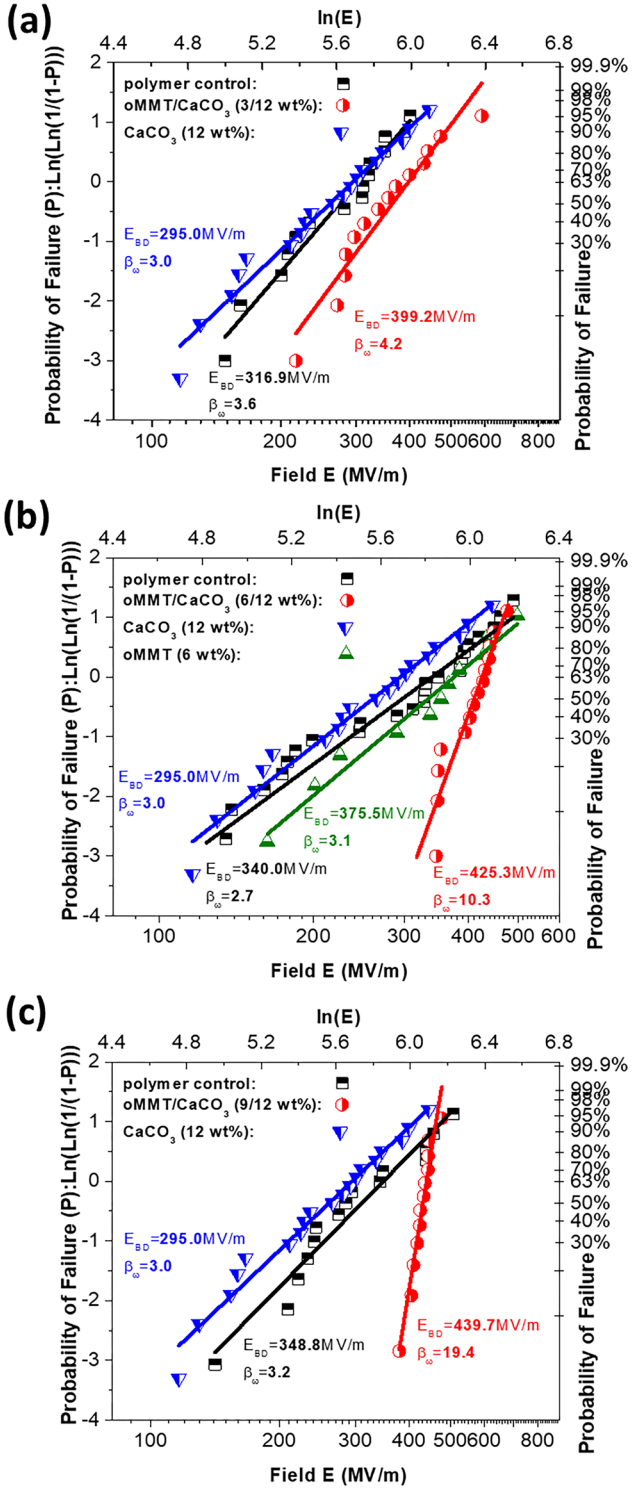

Figure 2. Weibull plots depicting the cumulative breakdown probability distribution as a function of applied electric field for the dual-filler composites with (a) 3 wt % oMMT and 12 wt % $CaCO_3$, (b) 6 wt % oMMT and 12 wt % $CaCO_3$, and (c) 9 wt % oMMT and 12 wt % $CaCO_3$; also included are the Weibull plots for the respective single-filler composites and the polymer controls.

DOI: 10.1021/acsanm.8b01127
ACS Appl. Nano Mater. 2018, 1, 4401−4407

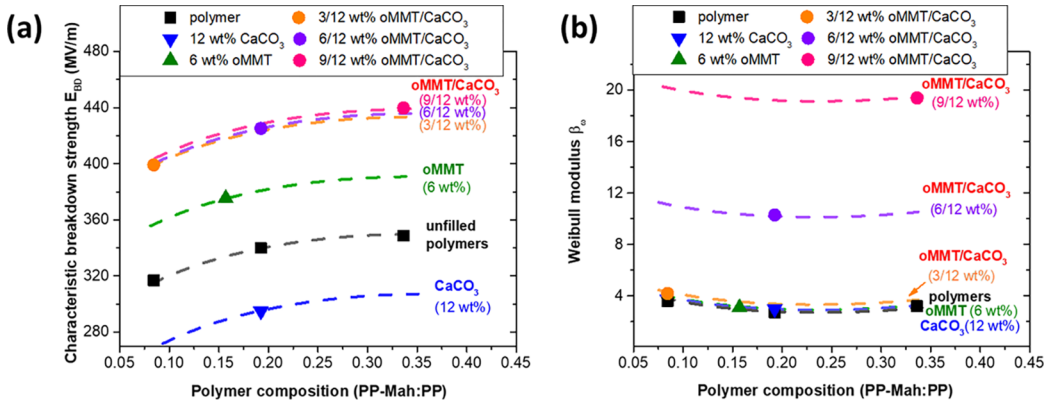

Figure 3. (a) Dielectric breakdown strength (E_{BD}) and (b) Weibull modulus (β_w) as a function of polymer-matrix composition for all samples. Symbols are the experimentally measured values, whereas the dashed lines show the expected breakdown for composites with the same filler contents but at different polymer compositions (i.e., different polymer blend ratios), i.e., we assume that the dielectric breakdown of the polymer-maxtrix in the composites changes with polymer compositionin the same manner as the measured breakdown of the respective unfilled polymers (black symbols and lines). Any differences in breakdown strength between the dashed lines measures the effect of different types of filler.

Table 1. Summary of Breakdown Performance, Crystallinity, and Polymer Composition for All Samples

samples	breakdown strength (MV/m) with 63.2% probability[a]	breakdown strength (MV/m) with 10% probability	β_w	ϕ_c (%)	PP−Mah/PP[b]
PP-1	316.9	169.6	3.6	19.5	0.084
PP-2	340.0	147.7	2.7	21.6	0.192
PP-3	348.8	172.6	3.2	24.3	0.336
PP-1/12%CC/3%OC[c]	399.2	233.6	4.2	17.4	0.084
PP-2/12%CC/6%OC	425.3	341.8	10.3	19.4	0.192
PP-3/12%CC/9%OC	439.7	391.5	19.4	22.3	0.336
PP/6%OC	375.5	181.7	3.1	20.7	0.157
PP/12%CC	295.0	139.3	3.0	20.0	0.192

[a]Electric field at 63.2% probability of failure corresponds to characteristic breakdown strength (E_{BD}). [b]The ratio between PP-Mah and PP is used to characterize the polymer composition of the samples for better evaluation of the filler effect. [c]OC stands for organoclay, or oMMT; CC stands for $CaCO_3$.

In addition to the increased E_{BD}, the structured hybrid nanocomposites also demonstrate improved distribution of breakdown failures. As shown in Figure 3b, the β_w shape parameter of the 6/12 wt % oMMT/$CaCO_3$ nanocomposite is 10.3, substantially larger than those of the respective polymer control and of the single-filler composites, which are measured to be ∼3−4; further increasing nanoclay concentration to 9 wt % in the dual-filler composite enhances β_w to 19.4. As a result of the larger β_w, these hybrid-filler nanocomposites exhibit remarkably better performance in the low field failures than the unfilled polymers and the single-filler composites. For instance, the breakdown field corresponding to 10% probability of failure is 342 MV/m for the 6/12 wt % oMMT/$CaCO_3$ nanocomposite, compared to 148 MV/m for the unfilled polymer, and to 139 and 182 MV/m for the 12 wt % $CaCO_3$ and 6 wt % oMMT single-filler nanocomposites, respectively (Table 1). Moreover, the entire population of failures for this structured hybrid nanocomposite lies above the characteristic breakdown field (E_{BD}) of the unfilled polymer and $CaCO_3$ polymer composite (Figure 2b). These considerations have important implications for practical applications, as it is often the low field breakdown strength that determines the operational electric field, rather than the characteristic Weibull strength.

The improved breakdown performance for the structured hybrid-filler composites is not related with the better filler dispersion or the polymer composition, as discussed before. Also, it is not due to any changes in the crystallinity or crystal phase of the polymer. As shown in Table 1, for each polymer composition, the crystallinities of the polymer nanocomposites (including both dual-filler and single-filler composites) and unfilled polymers are very similar to each other—less than 2% variation can be identified across all samples with the same polymer composition. Note that the PP used in this study is a PP terpolymer, which is then blended with PP-Mah as the polymer matrix. The inclusion of other-than-propylene monomers and Mah functional groups reduces the crystallinity (cf. $\phi_c \approx 20\%$ for the studied samples vs $\phi_c \approx 70-80\%$ for the isotactic PP), which also accounts for the lower-than-usual E_{BD} recorded for the unfilled PP polymers. Moreover, the polymers of the nanocomposites are exclusively crystallized into α-PP crystallites (Figure 1e); all specimens, regardless of with or without fillers, also show a similar multiple-melting behavior in the heating scans of differential scanning calorimetry (DSC) (with two separate melting peaks superimposed on a broad bump), indicating a similar distribution of crystalline morphologies (Figure S1). As a result, the enhanced high field properties in the hybrid nanocomposites definitively originate from the filler contribution and very likely from the specific hierarchical structure of the hybrid two-filler constructs.

Also as shown in Figure 3a, it is interesting to note that the E_{BD} increase in these hybrid nanocomposites with respect to the unfilled polymers, which represents the actual filler contribution, seems to be saturated at the lowest filler content; that is, a 25% improvement in E_{BD} is already achieved at 3/12 wt % oMMT/$CaCO_3$; further increasing oMMT content does not produce considerable additional E_{BD} improvement. Besides, these structured nanocomposites exhibit a much larger β_w than the rest of samples (single-filler composites and unfilled polymers), implying that the composite structure becomes more homogeneous with the addition of the two fillers (Figure 3b). These facts are reminiscent of typical percolation behaviors for polymer composites, and consequently, before further discussing any possible mechanisms for the observed improvement in

DOI: 10.1021/acsanm.8b01127
ACS Appl. Nano Mater. 2018, 1, 4401−4407

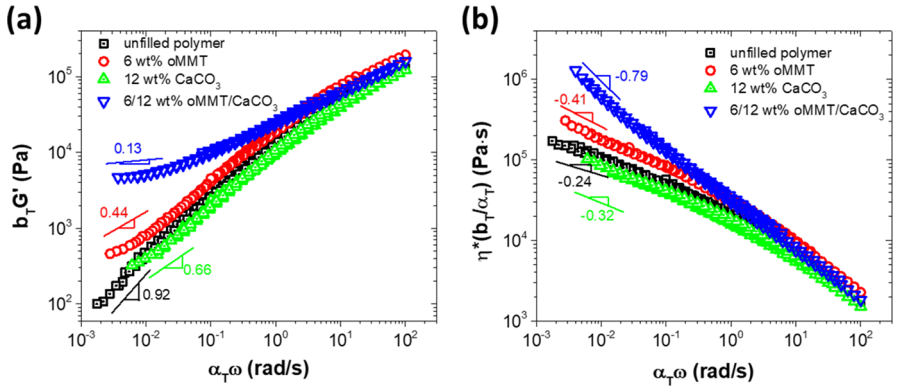

Figure 4. Melt state (a) storage modulus and (b) complex viscosity of the samples, superposed at T_m + 20 °C (20 °C above the melting temperature) of polymer to construct a rheological master curve.

breakdown performance, the linear dynamic rheological properties are reported below, to provide more insights into the structure of the hybrid filler.

The master curves of the storage modulus (G') and the complex viscosity (η^*) for the single-filler and dual-filler composites, as well as the unfilled polymer, in the melt state are shown in Figure 4. Since the interest here is to explore the filler structure as to whether an extended network is established, the low-frequency rheological behavior will be mainly discussed. In the low-frequency region, the slope of 0 for G' and −1 for η^* represent an ideal solid behavior, whereas the slope of 2 for G' and 0 for η^* characterize a liquid-like response.[24] As shown in Figure 4, the single-filler composite containing either 6 wt % oMMT or 12 wt % $CaCO_3$ exhibits a similar low-frequency viscoelastic performance to the unfilled polymer. The slightly increased G' and η^* arise from a certain level of filler−polymer interaction; nevertheless, the terminal behaviors of both single-filler composites are not qualitatively different from that of the unfilled polymer, indicating the absence of any extended filler networks; that is, the stress is mainly dissipated through the relaxation of polymer chains. In the dual-filler composite (6/12 wt % oMMT/$CaCO_3$) with the same amount of the fillers as in the single-filler composites, a clear solid-like response appears in the low-frequency region, as manifested by a quasi-plateau in G' and the deviation of η^* from a Newtonian viscosity plateau. The solid-like behavior reflects the formation of a filler network structure, within which the low-frequency rheological response is dominated by the deformation of the filler networks, instead of by the polymer chain relaxation.[23]

The solid-like behavior in the dual-filler composite cannot be ascribed to improved filler dispersion, as discussed before, nor to volume exclusion effect of the fillers (i.e., the addition of $CaCO_3$ as a cofiller would increase the effective concentration of oMMT in the composite, and vice versa). The latter can be clearly seen in Figure S2a,b. The single-filler composite with 16 wt % $CaCO_3$ or 9 wt % oMMT, which has higher filler concentration than the effective concentration of either filler in the 6/12 wt % oMMT/$CaCO_3$ composite, still behaves more like a liquid, implying that the solid-like rheological response of the dual-filler composite is not directly due to the increase in the total solid content. This can be further confirmed by the fact that the addition of an extra amount of $CaCO_3$ does not change the viscoelastic properties, that is, the 6/12 wt % oMMT/$CaCO_3$ and 6/16 wt % oMMT/$CaCO_3$ composites show an identical rheological behavior (Figure S2c), which again indicates that the solid-like behavior of the structured hybrid nanocomposites is not so much affected by the filler concentration but instead is primarily dictated by the interaction between the two fillers. It can be envisaged that $CaCO_3$ is bound to oMMT through physisorption or polymer-induced bridging interactions[23] (mediated by the coupling agents with one end tethered to $CaCO_3$ and the other end tethered to oMMT layers). The hybrid filler is thus stabilized and extends over large length scales, promoting the formation of a macroscopic network at a lower filler loading than otherwise needed.

Now let us return to the discussion of the electrical failures of the polymer composites. The E_{BD} degradation in the $CaCO_3$ composite indicates the presence of a dielectrically weak interface between these microfillers and the polymers. Shielding such interfaces with physisorbed platelet nanoclays is shown to mitigate this problem, as revealed by the improved breakdown performance of the structured hybrid-filler composites compared to the $CaCO_3$ composite. Even more interesting, the hybrid-filler composite E_{BD} improvement exceeds what either filler alone can achieve, CaCO3 or oMMT, implying synergies of the two fillers emerging upon the formation of this morphology. These observations are in concert with rheological measurement; both experimental results deviate from the prediction based on the weighted average of the mixture due to the synergistic effects between the fillers. These synergistic effects are believed to arise from the development of an extended filler structure, with the $CaCO_3$ particles located between and bridging the oMMT nanofillers. The assembled hybrid fillers are stabilized over a large length scale, leading to an early onset of percolation at low filler content. The initiation of a percolated structure can increase the structural and compositional homogeneity, resulting in an improved reliability for the structured nanocomposites when operating under high applied voltages, that is, narrowed distribution of failure fields (a large β_w). The breakdown strength, especially the low field failures, is also improved, which can be attributed to two reasons: (a) the extended structure of the hybrid filler can mitigate the failure propagation; for example, ion movement or treeing inception and development would be greatly frustrated within the labyrinthlike structure;[25] (b) since such morphology is established at relatively low filler loading, the space charges and other defects (ions, surfactants, chemical leftovers, etc.) introduced by the fillers are reduced in population, proportionally. In this respect, the structure tailoring for the hybrid filler is not unlike other strategies adopted in other studies, for example, improving the exfoliation of layered nanofillers, incorporating high aspect-ratio fillers,[26] or orienting nanofillers normal to *E*-

DOI: 10.1021/acsanm.8b01127
ACS Appl. Nano Mater. 2018, 1, 4401−4407

field,[19] all capitalizing on the morphology feature of an extended or even interwoven filler structure, so as to optimize the *E*-field distribution within polymer matrices and reinforce the barrier effects of polymer composites.[21] However, considering that many functional fillers are, like $CaCO_3$, not pertinent for high field endurance, this tailored hybrid-filler approach bears the promise of acquiring property improvements imparted by the filler/filler structuring, rather than the intrinsic filler properties, and without compromising E_{BD}; thus overcoming the common property trade-off for dielectric polymer composites.

In summary, structured PP/MMT/$CaCO_3$ nanocomposites are produced, with the MMT nanoclays predominantly distributed at the interfaces of the $CaCO_3$ particles. The breakdown performance of these structured hybrid nanocomposites surpasses that of the unfilled polymers and either single filler composite; this behavior is attributed to the particular structure of the hybrid filler: The MMT nanofillers physisorbed on the surfaces of the $CaCO_3$ can shield the dielectrically weak $CaCO_3$/PP interfaces, preventing low energy electrical failures; the $CaCO_3$ particles can bridge the nearby MMT nanofillers to form an extended hybrid-filler structure. The low-energy failure initiation and propagation can be greatly mitigated within this labyrinthlike structure. This specific multifiller composite morphology can be applied to other dielectric composite systems to achieve concurrent improvement of E_{BD} and enhancement in other thermophysical and dielectric properties.

■ ASSOCIATED CONTENT

Supporting Information

The Supporting Information is available free of charge on the ACS Publications website at DOI: 10.1021/acsanm.8b01127.

Experimental details, two-parameter Weibull statistics, DSC measurements of the single-filler/dual-filler polymer composites and the respective polymer controls, dynamic linear viscoelastic measurements for the composite and unfilled polymer samples, comparison of E_{BD} with mechanical properties (PDF)

■ AUTHOR INFORMATION

Corresponding Authors

*E-mail: bolipsu@gmail.com. (B.L.)
*E-mail: manias@psu.edu. (E.M.)

ORCID

Bo Li: 0000-0002-4890-8435
Evangelos Manias: 0000-0003-0705-0601

Present Addresses

‡Department of Chemical Engineering, University of Los Andes, Bogotá 111711, Colombia.
§Department of Chemistry, Aristotle University of Thessaloniki, Thessaloniki GR 54124, Greece.

Notes

The authors declare no competing financial interest.

■ ACKNOWLEDGMENTS

This work was supported by the National Science Foundation, as part of the Center for Dielectrics and Piezoelectrics under Grant Nos. IIP-1361571 and IIP-1361503. Additional support through CSC and ΓΓΕΤ fellowships is acknowledged by B.L. and P.I.X., respectively.

■ REFERENCES

(1) Tanaka, T.; Montanari, G.; Mulhaupt, R. Polymer Nanocomposites as Dielectrics and Electrical Insulation-Perspectives for Processing Technologies, Material Characterization and Future Applications. *IEEE Trans. Dielectr. Electr. Insul.* **2004**, *11*, 763−784.
(2) Nelson, J. K. *Dielectric Polymer Nanocomposites;* Springer: New York, NY, 2010.
(3) Dang, Z. M.; Yuan, J. K.; Zha, J. W.; Zhou, T.; Li, S. T.; Hu, G. H. Fundamentals, Processes and Applications of High-Permittivity Polymer−Matrix Composites. *Prog. Mater. Sci.* **2012**, *57*, 660−723.
(4) Ducharme, S. An Inside-Out Approach to Storing Electrostatic Energy. *ACS Nano* **2009**, *3*, 2447−2450.
(5) Zhang, X.; Shen, Y.; Zhang, Q.; Gu, L.; Hu, Y.; Du, J.; Lin, Y.; Nan, C. W. Ultrahigh Energy Density of Polymer Nanocomposites Containing $BaTiO_3$@TiO_2 Nanofibers by Atomic-Scale Interface Engineering. *Adv. Mater.* **2015**, *27*, 819−824.
(6) Li, B.; Xidas, P. I.; Triantafyllidis, K. S.; Manias, E. Effect of Crystal Orientation and Nanofiller Alignment on Dielectric Breakdown of Polyethylene/Montmorillonite Nanocomposites. *Appl. Phys. Lett.* **2017**, *111*, 082906.
(7) Yu, K.; Niu, Y.; Bai, Y.; Zhou, Y.; Wang, H. Poly(vinylidene fluoride) Polymer Based Nanocomposites with Significantly Reduced Energy Loss by Filling with Core-Shell Structured $BaTiO_3$/SiO_2 Nanoparticles. *Appl. Phys. Lett.* **2013**, *102*, 102903.
(8) Li, Q.; Zhang, G.; Liu, F.; Han, K.; Gadinski, M. R.; Xiong, C.; Wang, Q. Solution-Processed Ferroelectric Terpolymer Nanocomposites with High Breakdown Strength and Energy Density Utilizing Boron Nitride Nanosheets. *Energy Environ. Sci.* **2015**, *8*, 922−931.
(9) Li, Q.; Chen, L.; Gadinski, M. R.; Zhang, S.; Zhang, G.; Li, H. U.; Iagodkine, E.; Haque, A.; Chen, L. Q.; Jackson, T. N.; Wang, Q. Flexible High-Temperature Dielectric Materials from Polymer Nanocomposites. *Nature* **2015**, *523*, 576−579.
(10) Tomer, V.; Polizos, G.; Randall, C. A.; Manias, E. Polyethylene Nanocomposite Dielectrics: Implications of Nanofiller Orientation on High Field Properties and Energy Storage. *J. Appl. Phys.* **2011**, *109*, 074113.
(11) Tomer, V.; Manias, E.; Randall, C. A. High Field Properties and Energy Storage in Nanocomposite Dielectrics of Poly(vinylidene fluoride-hexafluoropropylene). *J. Appl. Phys.* **2011**, *110*, 044107.
(12) Li, B.; Camilli, C. I.; Xidas, P. I.; Triantafyllidis, K. S.; Manias, E. Structured Polyethylene Nanocomposites: Effects of Crystal Orientation and Nanofiller Alignment on High Field Dielectric Properties. *MRS Adv.* **2017**, *2*, 363−368.
(13) Tanaka, T.; Kozako, M.; Fuse, N.; Ohki, Y. Proposal of a Multi-Core Model for Polymer Nanocomposite Dielectrics. *IEEE Trans. Dielectr. Electr. Insul.* **2005**, *12*, 669−681.
(14) Li, Q.; et al. High Energy and Power Density Capacitors from Solution-Processed Ternary Ferroelectric Polymer Nanocomposites. *Adv. Mater.* **2014**, *26*, 6244−6249.
(15) Tomer, V.; Polizos, G.; Manias, E.; Randall, C. A. Epoxy-Based Nanocomposites for Electrical Energy Storage. I: Effects of Montmorillonite And Barium Titanate Nanofillers. *J. Appl. Phys.* **2010**, *108*, 074116.
(16) Polizos, G.; Tomer, V.; Manias, E.; Randall, C. A. Epoxy-Based Nanocomposites for Electrical Energy Storage. II: Nanocomposites with Nanofillers of Reactive Montmorillonite Covalently-Bonded with Barium Titanate. *J. Appl. Phys.* **2010**, *108*, 074117.
(17) Zhou, T.; Zha, J. W.; Cui, R. Y.; Fan, B. H.; Yuan, J. K.; Dang, Z. M. Improving Dielectric Properties of $BaTiO_3$/Ferroelectric Polymer Composites by Employing Surface Hydroxylated $BaTiO_3$ Nanoparticles. *ACS Appl. Mater. Interfaces* **2011**, *3*, 2184−2188.
(18) Cheng, Y.; Chen, X.; Wu, K.; Wu, S.; Chen, Y.; Meng, Y. Modeling and Simulation for Effective Permittivity of Two-Phase Disordered Composites. *J. Appl. Phys.* **2008**, *103*, 034111.
(19) Li, B.; Xidas, P.; Manias, E. High Breakdown Strength Polymer Nanocomposites Based on The Synergy of Nanofiller Orientation and Crystal Orientation for Insulation And Dielectric Applications. *ACS Appl. Nano Mater.* **2018**, *1*, 3520−3530.

DOI: 10.1021/acsanm.8b01127
ACS Appl. Nano Mater. 2018, 1, 4401−4407

(20) Chan, C. M.; Wu, J.; Li, J. X.; Cheung, Y. K. Polypropylene/Calcium Carbonate Nanocomposites. *Polymer* **2002**, *43*, 2981−2992.
(21) Fillery, S. P.; Koerner, H.; Drummy, L.; Dunkerley, E.; Durstock, M. F.; Schmidt, D. F.; Vaia, R. A. Nanolaminates: Increasing Dielectric Breakdown Strength of Composites. *ACS Appl. Mater. Interfaces* **2012**, *4*, 1388−1396.
(22) Van Oss, C. J.; Chaudhury, M. K.; Good, R. J. Interfacial Lifshitz-van der Waals and Polar Interactions in Macroscopic Systems. *Chem. Rev.* **1988**, *88*, 927−941.
(23) Xu, L.; Nakajima, H.; Manias, E.; Krishnamoorti, R. Tailored Nanocomposites of Polypropylene with Layered Silicates. *Macromolecules* **2009**, *42*, 3795−3803.
(24) Pötschke, P.; Abdel-Goad, M.; Alig, I.; Dudkin, S.; Lellinger, D. Rheological and Dielectrical Characterization of Melt Mixed Polycarbonate-Multiwalled Carbon Nanotube Composites. *Polymer* **2004**, *45*, 8863−8870.
(25) Li, B.; Manias, E. Increased Dielectric Breakdown Strength of Polyolefin Nanocomposites via Nanofiller Alignment. *MRS Adv.* **2017**, *2*, 357−362.
(26) Tang, H.; Sodano, H. A. Ultra High Energy Density Nanocomposite Capacitors with Fast Discharge Using $Ba_{0.2}Sr_{0.8}TiO_3$ Nanowires. *Nano Lett.* **2013**, *13*, 1373−1379.

DOI: 10.1021/acsanm.8b01127
ACS Appl. Nano Mater. 2018, 1, 4401−4407